PALEOMAGNETISM OF THE MOUNT BRUSSILOF MAGNESITE DEPOSIT AND ITS CAMBRIAN HOST ROCKS, SOUTHEASTERN BRITISH COLUMBIA (NTS 82 J/11, 12, 13)

D.T.A. Symons and M.T. Lewchuk, Department of Earth Sciences, University of Windsor, Windsor, Ontario

G.J. Simandl, Geological Survey Branch, British Columbia Ministry of Employment and Investment

D.F. Sangster, Geological Survey of Canada, Ottawa

Keywords: Mount Brussilof, paleomagnetism, magnesite, industrial minerals

INTRODUCTION

This study was undertaken to date the formation of the Mount Brussilof magnesite deposit. It is located about 35 km northeast of Radium Hotsprings in southeastern British Columbia (Figure 1). It is the only operating magnesite mine in Canada with proven and possible reserves of >40 Mt of >92% magnesia in 1980 (Simandl *et al.*, 1992). The deposit lacks minerals suitable for radiometric age dating and hence its age is uncertain. Geological relationships suggest that the magnesite postdates early diagenesis of the host Middle Cambrian Cathedral dolostone and pre-dates sparry dolomite, based on the field observations (Simandl and Hancock, 1996). Cross cutting field relationships indicate that sparry magnesite is at least slightly older than sparry dolomite. Restriction of magnesite to the Cathedral Formation, contrary to sparry dolomite which is present in both the Cathedral and younger overlying Eldon formations, further suggests that sparry magnesite may be linked to a specific time or depositional environment and possibly to the composition of the protolith. The deposit is hosted by the same rocks as nearby Mississippi Valley-type (MVT) lead-zinc deposits (Simandl *et. al.*, 1991; Nesbitt and Muehlenbachs, 1994). Most of the major MVT districts in North America have been successfully dated in the past few years using paleomagnetism, and most of these studies have been done in the paleomagnetic laboratory at the University of Windsor (Symons *et al.*, 1996).

Therefore it was decided to test the paleomagnetism of the Mount Brussilof deposit and its host rocks. The two prevailing hypothesis on the origin of the Mount Brussilof deposit are replacement of dolomitized permeable carbonates by magnesite due to interaction with a metasomatic fluid, assuming an appropriate aCa^{2+}/aMg^{2+} ratio, salinity, temperature, high fluid/rock ratio, *etc.* or post early-diagenetic recrystalliation of a magnesia-rich protolith of chemical, possibly evaporitic origin that may have consisted of fine-grained magnesite, hydromagnesite, huntite or other low temperature magnesia-bearing minerals. (Simandl and Hancock, 1996) The main difference between these hypotheses is the source of magnesia. The source is external in case of metasomatic replacement and *in situ* in the case of diagenetic recrystallization of magnesia-rich protolith.

Although this study was unsuccessful in directly dating the magnesite ore, as the first such attempt it is useful to describe the results obtained. The results provide evidence of a regional hydrothermal fluid flow that remagnetized the host rocks in Laramide time.

GEOLOGY

The Mount Brussilof mine is located in the Foreland tectonostratigraphic belt of the Canadian Cordillera about 400 metres east of the Cathedral escarpment (Simandl and Hancock, 1991; Figure 1). The escarpment separates deeper-water Middle Cambrian shales of the Chancellor Group on the west side from their shallow-water carbonate platform equivalents on the east side. The escarpment has been described variously as a paleoescarpment, an erosional facies change, a faulted facies change or a facies change on a fault ramp (Leech, 1966; Aitken, 1971, 1989; Ludwigsen, 1989; Aitken and McIlreath, 1990; Fritz, 1990).

East of the Cathedral escarpment, the stratigraphic sequence from oldest to youngest is: 1) >250 m of massive tan coarse-grained quartz sandstone of the Lower Cambrian Gog Formation; 2) 65-170 m of thin-bedded brown and green shale of the Middle Cambrian Naiset Formation; 3) ~340 m of buff and grey dolostone and limestone of the Cathedral Formation; 4) ~16 m of brown to grey fossiliferous shale of the Stephen Formation; 5) ~500 m of black, grey and buff dolostone of the Eldon and Pika formations and 6) green, purple and red shales with beige dolostone interbeds of the Middle Cambrian Arctomys Formation (Simandl and Hancock, 1991; Simandl *et al.*, 1992).

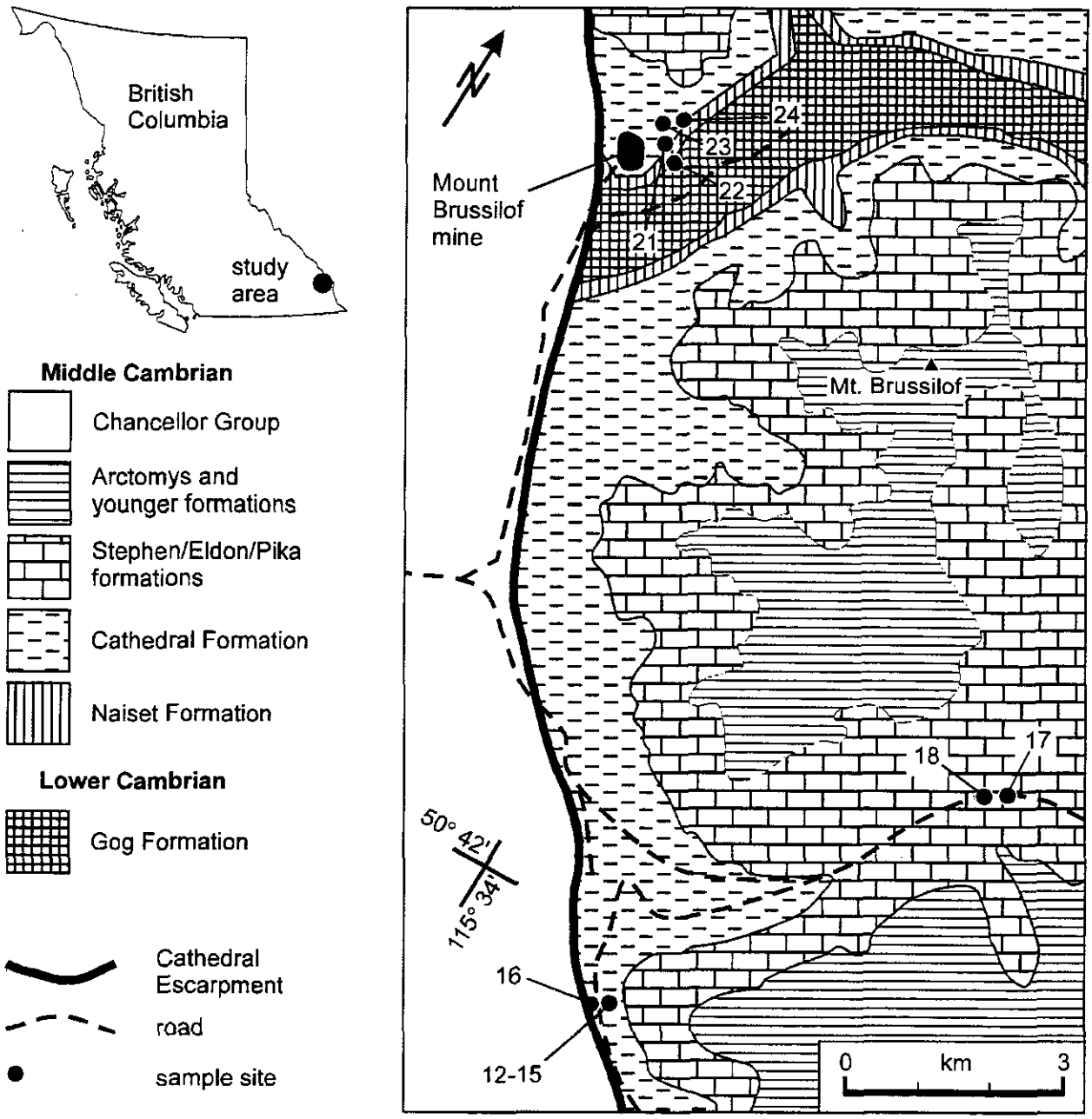

Figure 1. Location of the study area and sites (solid circles) with geology simplified from Simandl *et al.* (1992).

West of the escarpment the Chancellor Group is complexly folded and to the east forms a homoclinal sequence. The rocks cropping out in the proximity of the mine, immediately east of the Cathedral Escarpment strike 168/21 SW. Rocks south of the mine area strike approximately east-west and dip 10° to the south. (Simandl *et al.*, 1991).

The Mount Brussilof magnesite ore is composed of coarse, white to grey, sparry magnesite crystals in the lower Cathedral Formation. There is a small percentage of impurities such as dolomite, calcite, pyrite, ankerite and about a dozen other relatively uncommon minerals (White, 1972).

PALEOMAGNETIC METHODS

Drill cores from sites 1 to 11 and 16 to 20 were oriented by sun compass and sliced into specimens. Block samples from the remaining sites were oriented by magnetic compass and specimens were later drilled from them in the laboratory (Figure 1). The 409 specimens were stored for several months and then measured inside a three-layer steel magnetically-shielded room with a field of ~0.2 percent of the Earth's ambient magnetic field to allow viscous remanent magnetization (VRM) components to decay.

Remanence measurements were done on an automated Canadian Thin Films model DRM-420 cryogenic magnetometer that is one of the world's most efficient and sensitive for this type of research. After measuring the natural remanent magnetization (NRM) of each specimen, two or more specimens from each site were alternating field (AF) step demagnetized at 5, 10, 15, 20, 25, 30, 40, 50, 60, 80 and 100 milliTesla (mT) using a Sapphire Instruments model SI-4 demagnetizer. Next two or more specimens from each site were thermally step demagnetized at 250, 350, 400, 450, 500, 530, 555 and 580°C using a Magnetic Minerals model MM-1 demagnetizer. The remaining specimens from each site were AF demagnetized in four to six steps. Those with NRM intensities of $<2 \times 10^{-5}$ Ampere/metr (A/m) were started at 15 mT and the rest at 20 mT with steps of 10 or 20 mT up to 60 to 100 mT.

Saturation isothermal remanence magnetization (SIRM) analysis was done on 11 representative specimens by pulse magnetizing them in 11 direct field steps up to 900 mT using a Sapphire Instruments model SI-6 pulse magnetizer, and then AF demagnetizing them in six steps to 50 mT. A further nine specimens were pulse magnetized at 900 mT and then thermally demagnetized in nine steps to 670°C.

Characteristic remanent magnetization (ChRM) components were identified from the step demagnetization data using both orthogonal vector plots (Zijderveld, 1967) and the least-squares fitting method of Kirschvink (1980). Site mean and unit mean statistics were done using Fisher (1953) statistics. It is most convenient to group the results of these analyses by rock type for discussion.

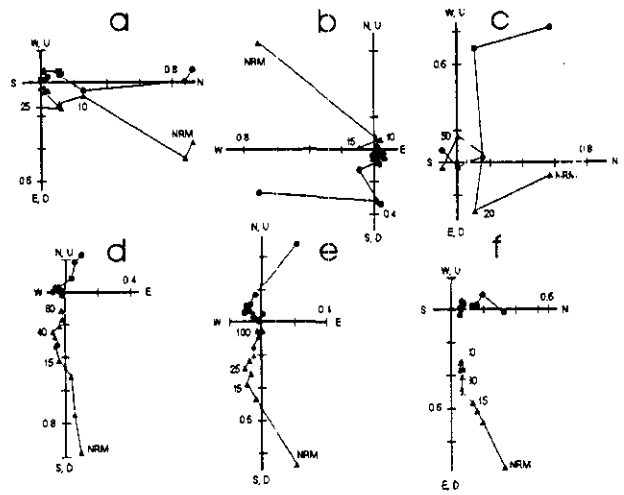

Figure 2. Orthogonal demagnetization diagrams showing example specimens on AF step demagnetization of: a) magnesite ore, site 1, $J_0 = 7.98 \times 10^{-5}$ A/m; b) magnesite ore, site 7, $J_0 = 4.61 \times 10^{-5}$ A/m; c) Gog sandstone, site 22, $J_0 = 1.20 \times 10^{-3}$ A/m; d) Cathedral dolostone, site 19, $J_0 = 1.51 \times 10^{-4}$ A/m; e) Cathedral dolostone, site 20, $J_0 = 1.29 \times 10^{-4}$ A/m; and, f) Eldon dolostone, site 17, $J_0 = 8.50 \times 10^{-5}$ A/m. The axes are north (N), east (E), south (S), west (W), up (U) and down (D). Circles (triangles) denote projections onto the horizontal (vertical) plane. The axes show the J/J_0 ratio. The AF steps are in millitesla (mT).

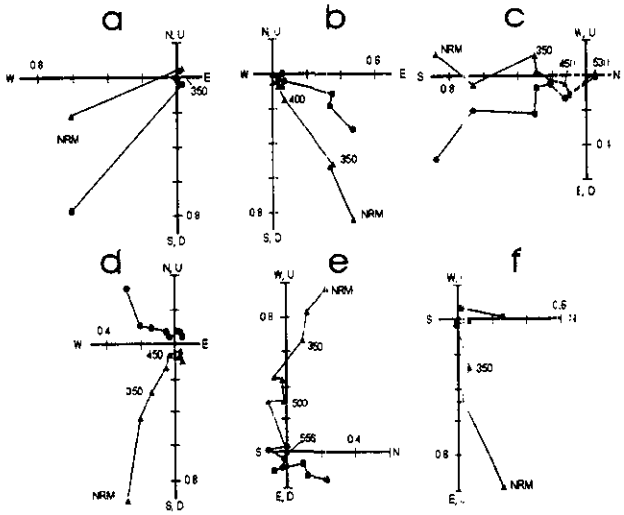

Figure 3. Orthogonal demagnetization diagrams showing example specimens on thermal step demagnetization of: a) magnesite ore, site 2, $J_0 = 3.62 \times 10^{-4}$ A/m; b) magnesite ore, site 6, $J_0 = 4.80 \times 10^{-4}$ A/m; c) Gog sandstone, site 22, $J_0 = 1.03 \times 10^{-3}$ A/m; d) Cathedral dolostone, site 19, $J_0 = 2.14 \times 10^{-4}$ A/m; e) Cathedral dolostone, site 21, $J_0 = 1.87 \times 10^{-3}$ A/m; and, f) Eldon dolostone, site 18, $J_0 = 4.88 \times 10^{-4}$ A/m. Conventions as in Figure 2 except the steps are in degrees Celsius (°C).

TABLE 1. SITE MEAN REMANENCE DIRECTIONS

Site	Unit	Strike	Dip	Sampling B	N	n	r	Demagnetizing Range H_{af}	°C	Decl. °	Incl. °	a_{95} °	k
1	m			6	11	6	1	15 - 25	250 - 400	323.2	30.0	14.7	18
2	m			6	12	6	0	15 - 25		47.6	-7.6	20.3	10
3	m			7	13	6	0	15 - 25	250 - 450	4.4	35.3	10.9	39
4	m			5	8	3	2	15 - 25		255.4	41.3	18.1	19
5	m			7	12	4	2	15 - 40		248.7	46.0	14.5	22
6	m			6	11								
7	m			7	12								
8	m			7	13	7	1	15 - 25		32.4	64.7	13.4	18
9	m			6	12	8	1	15 - 25		49.0	49.9	10.8	24
10	m			7	12								
11	m			7	13								
12	b*			6	47	47	0	20 - 80	250 - 530	344.1	74.9	5.4	157
13	b*			7	34	34	0	20 - 100	250 - 400	286.7	74.7	9.5	42
14	b*			4	22	22	0	15 - 80	250 - 350	312.8	79.0	12.3	57
15	s			2	18	15	0	20 - 100	500 - 555	181.0	-52.5	13.2	9
16	b*			13	24	23	0	20 - 130	250 - 450	358.9	71.2	10.4	17
17	e	52	16	6	14	14	0	20 - 100	250 - 400	10.7	75.1	4.2	92
18	e	57	10	5	11	11	0	20 - 100	250 - 350	338.1	79.1	5.6	68
19	c	132	81	7	12	11	0	20 - 100	250 - 400	315.0	76.0	7.9	35
20	c	159	13	6	17	17	0	20 - 80	250 - 400	292.8	71.0	3.4	111
21	c	297	30	4	14	6	2	15 - 60	500 - 530	345.9	76.9	14.5	16
22	g	168	30	4	18								
23	c	167	38	4	12	12	0	20 - 110	250 - 530	330.0	67.9	8.6	26
24	s			4	36								

Notes:

Geologic units are: Gog (g), Cathedral (c) and Eldon (e) formations; magnesite ore (m); breccia clasts (b) with the asterisk denoting that the site mean is derived from the clast mean directions; secondary dolomite (s). Strike and dip are given by a right-hand convention. Sampling gives the number of: cores or blocks (B); specimens measured (N); and specimen end points (n) and reversed end points (r) used to obtain the site mean. Demagnetizing range of alternating field intensities (H in millitesla) and temperatures (°C); the steps of specimen ChRM directions are averaged. Declination (Decl.), inclination (incl.), radius of cone at 95 percent confidence (a_{95}) in degrees (°C) of arc and precision parameter (k) from Fisher (1953).

RESULTS

Magnesite Ore

The 11 sites of magnesite ore were distributed quite uniformly along the mining faces of the Mount Brussilof open pit. The median NRM intensity of the 120 specimens is a very weak 2.7 x 10^{-5} A/m. On AF step demagnetization the NRM decays rapidly, giving consistent ChRM directions down to <3 x 10^{-6} A/m (Figure 2 a,b). Thermal step demagnetization also results in a rapid decay of the ChRM to <3 x 10^{-6} A/m by 450°C for most specimens without defining an obvious Néel or Curie temperature to identify the remanence carrier (Figure 3a). A few specimens with stronger NRM intensities appear to define a ChRM that is unblocked between about 350 and 500°C (Figure 3b). The SIRM acquisition curves show a steady increase up to 900 mT (Figure 4a) and slow decrease on AF step demagnetization (Figure 4b) that is typical of either goethite or hematite. These minerals, however, have not been observed in the ore in sufficient abundance to yield the observed intensities. Similarly, thermal step demagnetization of the SIRM shows no evidence of these minerals (Figure 4c). Thus the source of the remanence in the magnesite ore remains uncertain. Seven magnesite sites show some degree of clustering of their specimen ChRM directions (Table 1) but their mean directions are widely scattered (Figure 5a). The reason for this dispersion is also unclear.

Gog Formation

The 22 specimens from site 22 in the Gog sandstone have a strong median NRM intensity of 1.0 x 10^{-3} A/m. All undergo rapid AF demagnetization, reaching ~10% of their initial NRM intensity by 30 mT and giving inconsistent directions thereafter (Figure 2c). A few specimens appear to give consistent ChRM directions over a broad unblocking temperature spectrum (Figure 3c). Unfortunately, however, the 22 specimens give random ChRM directions, yielding no useful paleomagnetic data.

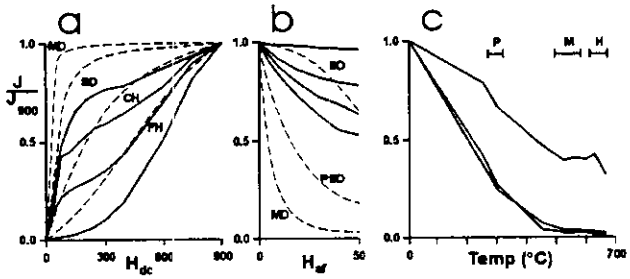

Figure 4. Saturation isothermal remanent magnetization (SIRM) curves for magnesite ore specimens showing: a) acquisition of SIRM; b) AF demagnetization of SIRM; and, c) thermal demagnetization of SIRM. J/J_{900} is the ratio of the measured remanence intensity to the SIRM intensity at 900 mT. H_{dc} and H_{af} are the applied direct and alternating fields in millitesla (mT). T is the temperature in degrees Celsius (°C). The dashed line curves are typical for single domain (SD), pseudosingle domain (PSD) and multidomain (MD) magnetite and for fine-grained (FH) and coarse-grained (CH) hematite from Dunlop (1973, 1981). P, M and H show the diagnostic temperature range in which pyrrhotite, magnetite and hematite, respectively, are magneticaly unblocked so that the J/J_{900} ratio decreases rapidly. The saturation intensities, J_{900}, for specimens from sites 1, 5, 6, 7, 9, 10, and 11 are 2.54, 2.05, 2.48, 57.0. 7.01, 7.02, and 16.6 x 10^{-3} A/m respectively.

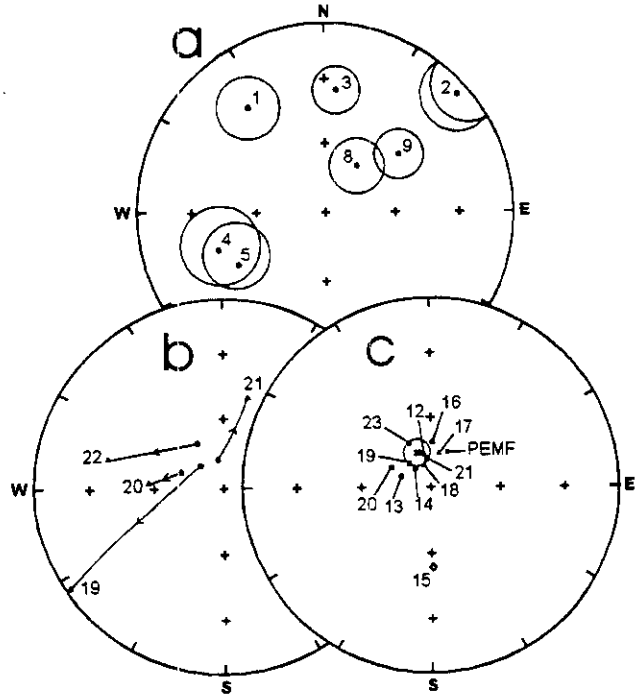

Figure 5. Equal-area stereograms showing the site mean ChRM directions for: a) magnesite ore; b) Cathedral dolostone before (circles) and after (triangles) tectonic tilt correction; and, c) all reliable host-rock sites before tilt correction. On (c) the rock types are Cathedral dolostone (square), Eldon dolostone (triangle), breccia clasts (circle), and secondary dolomite (diamond). The unit mean (x) is circumscribed by its cone of 95% confidence. The star is the present Earth's magnetic field direction.

Cathedral Formation

FOLD TEST

Sites 19, 20, 21 and 23 are in fine-grained dolostones and limestones of the Cathedral Formation with dips ranging from 13° to 80°. They were collected to provide a paleomagnetic fold test (Graham, 1949). If their ChRM directions are better grouped after tilt correction, then the ChRM predates folding and is likely primary, and if the converse is true then the ChRM is postfolding and secondary. The 55 specimens from the four sites have a median NRM intensity of 1.7 x 10^{-4} A/m. AF step demagnetization up to ~20 mT removes a VRM that appears to record mostly the present Earth's magnetic field direction, and from ~20 mT to 100 mT a well-defined ChRM is isolated (Figure 2d,e). Thermal step demagnetization results in a steady decay of the NRM intensity down to ~10% at ~450°C, followed by constant or slightly increased intensities thereafter (Figure 3d). On both AF and thermal step demagnetization most ChRMs give normal directions that are directed northerly and steeply downwards except for a few from site 21 that are reversed, being antiparallel and upwards to the south (Figure 3e).

The SIRM acquisition curves for the Cathedral specimens show a rapid initial increase up to ~300 mT which is indicative of either magnetite or pyrrhotite, followed by a slow increase from ~300 mT to 900 mT which suggests that goethite or hematite is present (Figure 6a). AF demagnetization of the SIRM yields decay rates that show that the magnetite or pyrrhotite is in the single domain to pseudosingle domain size range (Figure 6b) and thermal demagnetization of the SIRM gives unblocking temperatures that suggest that pyrrhotite, magnetite and hematite are present (Figure 6c).

All four sites of the Cathedral host rocks give well-clustered specimen ChRM directions that yield reliable site mean directions (Table 1, Figure 5b). Before tilt correction, they are tightly clustered with a precision parameter (k, Fisher, 1953) of k_u=111 whereas after tilt correction the ChRM directions are widely dispersed with a k_c value of 3.4 (Table 2). Using the fold test of McElhinny (1964), this results in a k ratio (k_u/k_c) of 32.6 that is very much greater than the 99% confidence comparison statistic of 8.47. Thus the fold test shows clearly that the ChRM is post-folding in origin with >>99% confidence, as does the more sophisticated test of McFadden and Jones (1981).

BRECCIA TEST

South of the Mount Brussilof mine there is a chevron fold in the Cathedral dolostones next to the Cathedral escarpment. In the nose of the fold is an "I saddle reef" trough of sparry dolomite with numerous clasts of the host rock. Sites 12, 13, 14, and 16 are located in different areas of the "reef" structure and provided 128 specimens from 30 breccia clasts. The breccia test asserts that the

TABLE 2. UNIT MEAN DIRECTIONS

Unit			Sites	N	Decl. °	Incl. °	a_{95} °	k
A	Cathedral Fm. -	uncorrected	19-21, 23	4	319.3	73.9	8.7	111
B	Cathedral Fm. -	corrected	19-21, 23	4	280.2	52.1	59.2	3.4
C	Eldon Fm. -	uncorrected	17, 18	2	357.0	77.6		198
D	A + C -	uncorrected	17-21, 23	6	329.9	75.7	6.8	98
E	B + Eldon Fm. -	corrected	17-21, 23	6	283.9	69.1	38.5	4.0
F	Breccia clasts		12-14, 16	4	328.9	76.7	10.1	83
G	Secondary dolomite		15	1	1.0	52.5		
H	F + G		12-16	5	341.7	72.6	13.7	32
I	All sites -	uncorrected	12-21, 23	11	335.8	74.4	6.2	54

Notes: N - number of site mean ChRM directions. Other abreviations as in Table 1

clasts will have random ChRM directions if they retain their pre-brecciation magnetization and aligned directions if they have been remagnetized since brecciation. The 128 specimens have a median NRM intensity of 8.1 x 10^{-4} A/m. This is much more intense than the other Cathedral dolostone specimens, suggesting that a more intense remagnetization ioccurred.

After removal of a VRM by about 20 mT, AF step demagnetization isolates either a well-defined normal ChRM direction or an initial normal ChRM that swings to a reverse ChRM direction (Figure 7a,b). The clast specimens respond more erratically to thermal step magnetization with most giving a normal ChRM direction up to ~450°C and then defining an erratic direction in magnetite up to ~570°C in the residual 5% of NRM intensity (Figure 8a). Two thermally demagnetized specimens give remagnetization circles towards the reversed ChRM direction but do not reach an end point before becoming erratic. The SIRM acquisition curves show the rapid initial rise to 300 mT that is attributable to either magnetite or pyrrhotite and then a slow rise to 900 mT from goethite or hematite (Figure 9a). Alternatively, the curves show a steady rise denoting the presence of goethite or hematite only. AF demagnetization of the SIRM indicates that the magnetite or pyrrhotite is single domain to pseudosingle domain in character (Figure 9b). The SIRM thermal demagnetization results indicate the presence of pyrrhotite and hematite (Figure 9c).

The several ChRM directions for each clast were averaged to get the clast mean directions which were mostly well clustered (Table 3). When necessary, reverse directions were switched to their antiparallel normal direction to compute the mean directions. The mean directions of the four sites form a coherent directional cluster, as do the clast directions when grouped irrespective of site (Table 3). The high degree of clustering yields a negative breccia test, meaning that the clasts were remagnetized when the breccia was formed or at some later date.

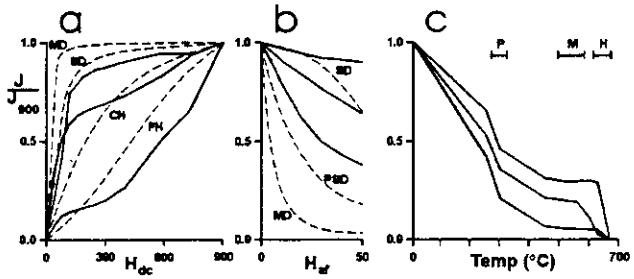

Figure 6. Saturation Isothermal Remanent Magnetization curves for Cathedral and Eldon dolostone specimens from sites 17, 17, 19, 20, 21 and 23 with J_{900} intensities of 3.05, 1.98, 2.52, 1.66, 4.59 and 5.24 x 10^{-2} A/m respectively. Conventions as in Figure 4.

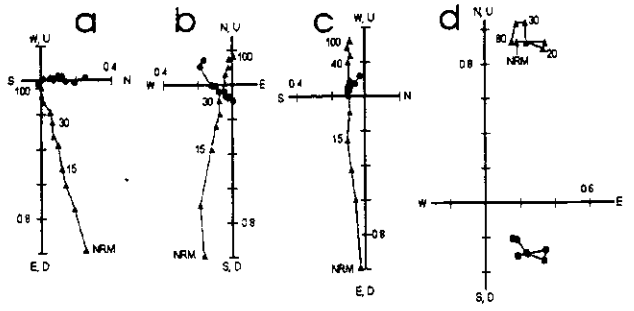

Figure 7. Orthogonal demagnetization diagrams showing example specimens on AF step demagnetization of: a) dolostone breccia clast, site 13, J_0 = 3.51 x 10^{-4} A/m; b) dolostone breccia clast, site 14, J_0 = 7.55 x 10^{-4} A/m; and, c) sparry dolomite, site 15, J_0 = 1.73 x 10^{-5} A/m. Conventions as in Figure 2.

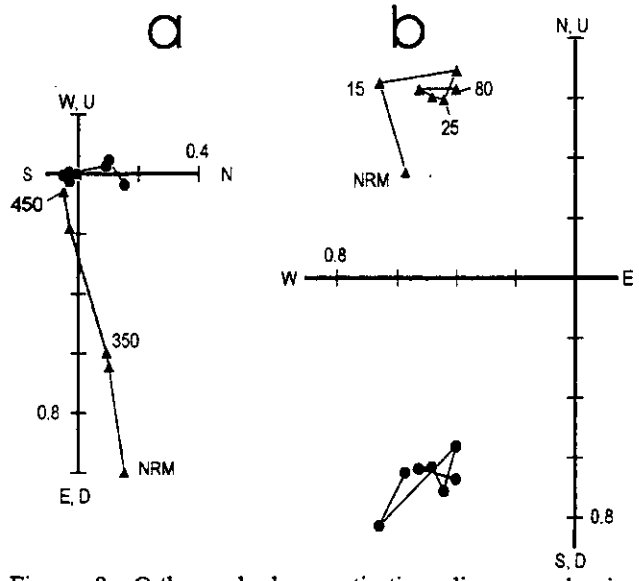

Figure 8. Orthogonal demagnetization diagrams showing example specimens on thermal step demagnetization of: a) dolostone breccia clast, site 12, J_0 = 2.39 x 10^{-3} A/m; and, b) sparry dolomite, site 15, J_0 = 2.38 x 10^{-3} A/m. Conventions as in Figure 3.

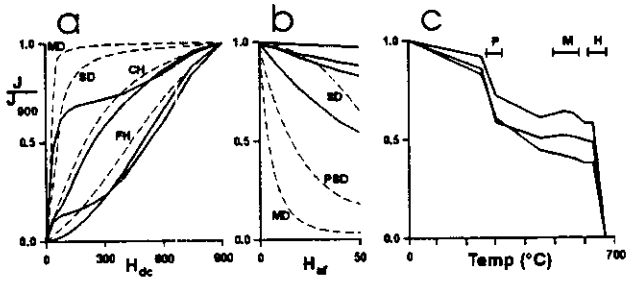

Figure 9. Saturation Isothermal Remanent Magnetization curves for dolostone breccia clast and secondary sparry dolomite specimens from sites 12, 13, 14, 15, 15, 16 and 16 with J_{900} intensities of 14.1, 7.58, 13.5, 21.6, 7.39, 21.9 and 28.9 x 10^{-2} A/m, respectively. Conventions as in Figure 4.

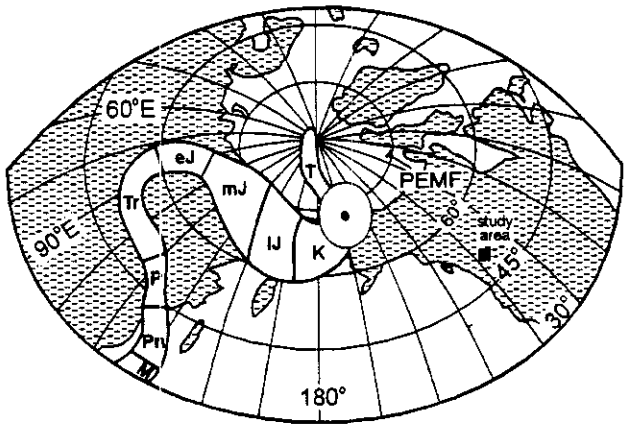

Figure 10. Apparent polar wander path for the North American craton with the host rock pole position of this study. The path for the Mississippian (M), Pennsylvanian (Pn), Permian (P), Triassic (Tr), and Early Jurassic (eJ) is from Van der Voo (1990); the path for the Middle Jurassic (mJ) and Late Jurassic (lJ) is simplified from Van der Voo (1992); and, the path for the Cretaceous (K) and Tertiary (T) is from Irving and Irving (1982). The pole is circumscribed by its oval of standard deviation, and the C pole from modern weathering is next to the present pole of the Earth's magnetic field (PEMF).

TABLE 3. REMANENCE DATA FOR BRECCIA CLASTS

Site Clast	N	n	Decl °	Incl °	a_{95} °	k
12-1	10	10	344.5	77.4	1.5	976
2	6	6	356.3	79.3	1.6	1666
3	9	9	342.5	75.1	2.7	383
4	6	6	333.2	74.7	2.8	594
5	7	7	319.6	71.1	3.6	288
6	9	9	7.3	67.7	1.3	1485
A		*6	344.1	74.9	5.4	157
13-1	8	8	284.4	70.9	4.8	133
2	4	4	308.9	71.6	12.5	55
3	5	5	324.4	81.2	5.4	203
4	6	6	224.9	75.6	7.9	74
5	4	4	287.6	75.5	11.3	67
6	4	4	247.5	65.7	7.9	137
7	3	3	322.8	62.0	24.9	26
A		*7	286.7	74.7	9.5	42
14-1	6	6	287.3	85.4	3.4	400
2	3	3	327.1	66.5	4.5	753
3	7	7	295.7	74.0	9.4	42
4	6	6	341.6	87.9	4.3	237
A		*4	312.8	79.0	12.3	57
16-1	3	2	168.2	-62.5		
2	2	2	192.6	-62.8		
3	2	2	182.7	-58.6		
4	2	2	11.8	81.7		
5	2	2	287.8	77.4		
6	1	1	134.9	-71.1		
7	2	2	180.6	-59.8		
8	3	3	187.2	-63.8	10.4	141
9	1	1	315.1	50.9	5.2	557
10	3	3	291.2	76		
11	2	2	162.6	-63.7		
12	1	1	173.7	-61.4		
13	1	1	99.6	52.8		
A		*13	358.9	71.2	10.4	17
All	30		333.7	75.1	5.4	25

Notes: N, n - number of specimens measured and used in clast average. * - number of clast mean directions averaged. Other abbreviations as in Table 1.

Eldon Formation

Sites 17 and 18, yielding 25 specimens with a median NRM intensity of 1.1 x 10^{-4} A/m, were collected from gently dipping dolostone of the Eldon Formation. Their behaviour on AF and thermal step demagnetization is essentially the same as found for the Cathedral dolostone specimens except that only normal ChRM directions were isolated (Figures 2f and 3f). The one SIRM acquisition curve suggests the presence of either goethite or hematite (Figure 6a) and thermal demagnetization of the SIRM shows unblocking in both the goethite (70-130°C) and hematite (600-675°C) range (Figure 6c). Note, however, that goethite can dehydrate to hematite on heating to about 350°C (Dekkers, 1990). Both sites give coherent site mean ChRM directions (Table 1).

Secondary Dolomite

Secondary dolomite was sampled at site 15 in the breccia zone and at site 24 next to the Mount Brussilof ore zone. The 54 specimens have a very weak median NRM intensity of only 2.0 x 10^{-5} A/m. At site 15 the more intense specimens swing from normal to a reverse ChRM, whereas the weaker specimens are virtually unchanged in either direction or intensity suggesting minor goethite or hematite (Figure 7c,d). In contrast, the specimens from site 24 show moderate to rapid rates of

demagnetization but isolate normal ChRM directions. Thermal step demagnetization of site 15 specimens isolates first a normal ChRM direction up to ~400°C and then a reversed direction at higher temperatures (Figure 8b). The specimens from site 24 define part of a normal to reverse remagnetization great circle, but define neither end point. The SIRM acquisition and demagnetization curves for a site 15 specimen are typical for fine-grained goethite or hematite, with the SIRM thermal demagnetization curve showing clearly that hematite is present (Figure 9). The specimens from site 15 give a reasonable site mean direction (Table 1), but those from site 24 are too widely scattered.

POLE POSITION OF THE HOST ROCKS

Useful site mean remanence directions have been obtained from four sites in the Cathedral Formation (sites 19, 20, 21 and 23), two in the Eldon Formation (sites 17 and 18), four in remagnetized breccia clasts (sites 12, 13, 14 and 16), and one in secondary dolomite (site 15). The negative fold and breccia tests both confirm that the remanence is post-folding in origin and, therefore, that the site mean ChRM directions should not be corrected for tilt. When these 11 sites are plotted together, they form a coherent population that has a unit mean direction of 335.8°, 74.4° (N=11, a_{95}=6.2°, k=54) (Figure 5c, Table 2). This unit mean gives a pole position of 159.5°W longitude, 73.2°N latitude (dp=10.2°, dm=11.2°, semi-axes of the oval of 95% confidence (Fisher, 1953)). This pole falls directly atop the Late Cretaceous portion of the apparent polar wander path (APWP) for the North American craton (Figure 10).

DISCUSSION

Extending northwestward for about 300 km from Mount Brussilof and southeastward for about 100 km is an area containing hydrothermal dolomites that is about 50 km wide along the northeastern side of the Cathedral escarpment. The sparry dolomite occurs as stratabound lenses, veins and irregular masses, with an earlier light gray, dark brown-black planar dolomite. Westervelt (1979) argued that the dolomite sheets were folded and faulted during the Laramide orogeny and thus predate the Late Jurassic. Yao and Demicco (1995) noted that Cambrian limestone boulders in Ordovician shales are unaltered whereas those on a Late Devonian erosional surface are dolomitized, suggesting that dolomitization occurred between the Ordovician and Late Devonian. They tied the dolomitization to a regional fluid flow event during Silurian to Devonian time from orogenic uplift in the Purcell anticlinorium and Kootenay arc on the west side of the escarpment (Okulitch, 1985). Based on field data from the Mount Brussilof area and available published information on MVT deposits, Simandl *et al.* (1991) pointed to a possible genetic link between the Mount Brussilof deposit and the Monarch-Kicking Horse and other MVT deposits in the secondary dolomite zone, suggesting also that they may be equivalent in age. Based on limited fluid inclusion salinities, homogenization temperatures, and $d^{18}O$, $d^{13}C$ and dD values, Nesbitt and Muehlenbachs (1994, 1995) further suggested that the dolomites and ore deposits were formed during a Late Devonian to pre-Laramide paleoflow event.

Contrasting with the preceding views for fluid flow in the Western Canada Sedimentary Basin (WCSB), several lines of evidence support a major Laramide paleoflow event in the WCSB. Oliver (1992), in an overview of interior North America, summarized extensive evidence for correlating regional fluid flows from orogenic events to the formation of petroleum deposits, dolomitization, MVT deposits and remagnetization of carbonate sediments. Qing and Mountjoy (1992, 1994) have provided extensive geologic, petrologic and geochemical data supporting a major Laramide paleoflow event in the WCSB. Machel *et al.* (1995) have used organic geochemistry to support a Laramide flow event. A mathematical hydrogeologic model for Laramide fluid flow in the WCSB has been given by Garven (1985). Paleomagnetic studies have shown that all major MVT deposits studied to date are coeval with a major adjacent orogenic event and that the Pine Point MVT ores in the WCSB are Laramide in age (Symons et al., 1993, 1996). Also, Enkin (1995) has reported that Paleozoic dolostones in the Front Ranges to the east of the secondary dolomite zone carry a Laramide remanence.

The results of this study provide strong evidence that at least some dolomitization is post-folding and therefore Laramide or Late Cretaceous to early Paleocene in age. The paleomagnetic data can not discriminate between metasomatic replacement or recrystallization theories for the origin of the magnesite ore. The source of the remanance in the magnesite ore remains uncertain. Although seven magnesite sites show some degree of clustering of their ChRM directions, their mean directions are widely scattered. One can only speculate about the reasons for this scatter. It may be linked to lower temperatures of recrystalization of magnesite relative to dolomite. Magnesite rock could have been relatively impermeable to Laramide fluids and therefore its paleomagnetic signature was not completely reset. Future work on other magnesite deposits that are less pure may resolve the age issue.

ACKNOWLEDGEMENTS

The authors thank Brock Symons who prepared the specimens; Praba Balasingham who measured the specimens; Heinz Fergen, Mine Manager and Baymag Mines Co. Ltd. who provided access to the mine; and the Natural Sciences and Engineering Research Council of Canada for research funding. The manuscript was reviewed by K.D. Hancock and Dr. David Lefebure of B.C. Geological Survey.

REFERENCES

Aitken, J.D. (1971): Control of Lower Paleozoic Sedimentary Facies by the Kicking Horse Rim, Southern Rocky Mountains, Canada; *Bulletin of Canadian Petroleum Geology*, Volume 19, pages 557-569.

Aitken, J.D. (1989): Birth, Growth and Death of the Middle Cambrian Cathedral Lithosome, Southern Rocky Mountains; *Bulletin of Canadian Petroleum Geology*, Volume 37, pages 316-333.

Aitken, J.D. and McIlreath, I.A. (1990): Comment on "The Burgess Shale: Not in the Shadow of the Cathedral Escarpment"; *Geoscience Canada*, Volume 17, pages 111-115.

Dekkers, M.J. (1990): Magnetic Properties of Natural Goethite - III. Magnetic Behaviour and Properties of Minerals Originating from Goethite Dehydration During Thermal Demagnetization; *Geophysical Journal International*, Volume 103, pages 233-250.

Dunlop, D.J. (1981): The Rock Magnetism of Fine Particles; *Physics of the Earth and Planetary Interior*, Volume 26, pages 1-26.

Dunlop, D.J. (1993): Thermoremanent Magnetization in Submicroscopic Magnetite; *Journal of Geophysical Research*, Volume 78, pages 7602-7613.

Enkin, R.J. (1995): Paleomagnetic Remagnetization Constraints on Tectonics and Thermal/Fluid History in the Canadian Rockies; *International Union of Geology and Geophysics*, XXI General Meeting, Abstract GAB31C-11, page B119.

Fisher, R.A. (1953): Dispersion on a Sphere; *Proceedings of the Royal Society of London*, Volume A217, pages 295-305.

Fritz, W.H. (1990): Comment: In Defence of the Escarpment near the Burgess Shale Fossil Locality; *Geoscience Canada*, Volume 17, pages 106-110.

Garven, G. (1985): The Role of Regional Fluid Flow in the Genesis of the Pine Point deposit, Western Canadian Sedimentary Basin; *Economic Geology*, Volume 80, pages 307-324.

Graham, J.W. (1949): The Stability and Significance of Magnetism in Sedimentary rocks; *Journal of Geophysical Research*, Volume 54, pages 131-167.

Irving, E. and Irving, G.A. (1982): Apparent Polar Wander Paths, Carboniferous through Cenozoic and the assembly of Gondwana; *Geophysical Surveys*, Volume 5, pages 141-188.

Kirschvink, J.L. (1980): The Least-squares Line and Plane and the Analysis of Palaeomagnetic Data; *Geophysical Journal of the Royal Astronomical Society*, Volume 62, pages 699-718.

Leech, G.B. (1966): Kananaskis Lakes; *Geological Survey of Canada*, Open File 634.

Ludwigsen, R. (1989): The Burgess Shale: Not in the Shadow of the Cathedral Escarpment; *Geoscience Canada*, Volume 16, pages 139-154.

Machel, H.G., Cavell, P.A. and Patey, K.S. (1995): Carbonate Diagenesis During Tectonic Expulsion of Fluids into the Western Canada Sedimentary Basin; *Lithoprobe Report 47*, pages 254-263.

McElhinny, M.W. (1964): Statistical Significance of the Fold test in Palaeomagnetism. *Geophysical. Journal of the Royal Astronomical Society*, Volume 8, pages 338-340.

McFadden, P.L. and Jones, D.L. (1981): The Fold Test in Palaeomagnetism; *Geophysical Journal of the Royal Astronomical Society*, Volume 67, pages 53-58.

Nesbitt, B.E. and Muehlenbachs, K. (1994): Paleohydrogeology of the Canadian Rockies and Origins of Brines, Pb-Zn Deposits and Dolomitization in the Western Canada Sedimentary Basin; *Geology*, Volume 22, pages 243-246.

Nesbitt, B.E. and Muehlenbachs, K. (1995): Regional Fluid Processes in the Generation of Magnesite, Talc and MVT Mineralization in the Canadian Rockies and Western Canada Sedimentary Basin; *Society of Economic Geologists*, St. Louis, Missouri Meeting, Extended Abstracts, pages 219-221.

Okulitch, A.V. (1985): Paleozoic Plutonism in Southeastern British Columbia; *Canadian Journal of Earth Sciences*, Volume 22, pages 1409-1424.

Oliver, J.E. (1992): The spots and stains of plate tectonics; *Earth Science Reviews*, Volume 32, pages 77-106.

Qing, H. and Mountjoy, E. (1992): Large-Scale Fluid Flow in the Middle Devonian Presqu'ile Barrier, Western Canada Sedimentary Basin; *Geology*, Volume 20, pages 903-906.

Qing, H. and Mountjoy, E. (1994): Formation of Coarsely Crystalline, Hydrothermal Dolomite Reservoirs in the Presqu'ile Barrier, Western Canada Sedimentary Basin; *Bulletin of the American Association of Petroleum Geology*, Volume 78, pages 55-77.

Simandl, G.J. and Hancock, K.D. (1991): Geology of the Mount Brussilof Magnesite Deposit, Southeastern British Columbia; *in* Geological Fieldwork 1990, *B.C. Ministry of Energy, Mines and Petroleum Resources*, Paper 1991-1, pages 269-278.

Simandl, G.J. and Hancock, K.D. (1996): Sediment-hosted Sparry Magnesite Deposits; *in:* New Mineral Deposit Models of the Cordillera; 1996 Cordilleran Roundup Short Course, British Columbia Geological Survey, pages W1-W9.

Simandl, G.J., Hancock, K.D., Hora, Z.D., MacLean, M.E. and Paradis, S. (1991): Regional Geology of the Mount Brussilof Carbonate-hosted Magnesite Deposit, Southeastern British Columbia, Canada; *in* Industrial Minerals of Alberta and British Columbia, Proceedings, Banff, Alberta, *Alberta Geological Survey* and *Alberta Research Council*, Information Series 115, pages 57-65.

Simandl, G.J., Hancock, K.D., Fournier, M., Koyanagi, V.M., Vilkos, V., Lett, R. and Colbourne, C. (1992): Geology and Major Element Geochemistry of the Mount Brussilof Magnesite Area, Southeastern British Columbia (82J/12, 13); *B.C. Ministry of Energy, Mines, and Petroleum Resources*, Open File 1992-14, 14 pages.

Symons, D.T.A., Pan, H., Sangster, D.F. and Jowett, E.C. (1993): Paleomagnetism of the Pine Point Zn-Pb Deposits; *Canadian Journal of Earth Sciences*, Volume 30, pages 1028-1036.

Symons, D.T.A., Sangster, D.F. and Leach, D.L. (in press): Paleomagnetic dating of Mississippi Valley-type Pb-Zn-Ba deposits; *in* Carbonate-hosted Lead-Zinc Deposits, D.F. Sangster, Editor, *Society of Economic Geologists*, Special Volume 4.

Van der Voo, R. (1990): Phanerozoic Paleomagnetic Poles from Europe and North America and Comparisons with Continental Reconstructions; *Reviews of Geophysics*, Volume 28, pages 167-206.

Van der Voo, R. (1992): Jurassic Paleopole Controversy: Contributions from the Atlantic-bordering Continents; *Geology*, Volume 20, pages 975-978.

Westervelt, T. (1979): Structural Superposition in the Lake O'Hara Region, Yoho and Kootenay National Parks, British Columbia, Canada; unpublished Ph.D. thesis, *University of Wyoming*, Laramie, 264 pages.

White, G.P.E. (1972): Mineralogy of the Baymag Mines Ltd. Magnesite Prospect, South Kootenay Area, B.C.; *Acrers Western Limited*, unpublished report, 17 pages.

Yao, Q. and Demicco, R.V. (1995): Paleoflow Patterns of Dolomitizing fluids and Paleohydrogeology of the Southern Canadian Rocky Mountains: Evidence from Dolomite Geometry and Numerical Modelling; *Geology*, Volume 23, pages 791-794.

Zijderveld, J.D.A. (1967): A.C. Demagnetization of Rocks: Analysis of Results; *in* Methods in Paleomagnetism, D.W. Collinson, K.M. Creer, and S.K. Runcorn, Editors, Elsevier, Amsterdam, pages 254-286.